Received: 22 December 2023 | Revised: 27 March 2024 | Accepted: 29 March 2024

DOI: 10.1002/esp.5850

RESEARCH ARTICLE

ESPL WILEY

# Impounded sediment and dam removal: Erosion rates and proximal downstream fate

Mathias J. Collins[1] | Matthew E. Baker[2] | Matthew J. Cashman[3] | Andrew Miller[2] | Stephen Van Ryswick[4]

[1]National Marine Fisheries Service, National Oceanic and Atmospheric Administration, Gloucester, Massachusetts, USA

[2]Department of Geography and Environmental Systems, University of Maryland—Baltimore County, Baltimore, Maryland, USA

[3]U.S. Geological Survey, Water Mission Area, Baltimore, Maryland, USA

[4]Maryland Geological Survey, Department of Natural Resources, Baltimore, Maryland, USA

**Correspondence**
Mathias J. Collins, National Marine Fisheries Service, National Oceanic and Atmospheric Administration, 55 Great Republic Drive, Gloucester, MA, 01930, USA.
Email: mathias.collins@noaa.gov

**Funding information**
National Marine Fisheries Service NOAA, Grant/Award Numbers: NA13NMF4630127, NA16NMF4630317, NA19NMF4630270; U. S. Fish and Wildlife Service, Grant/Award Number: F18AC00022

## Abstract

Sediment management is an important aspect of dam removal projects, often driving costs and influencing community acceptance. For dams storing uncontaminated sediments, downstream release is often the cheapest and most practical approach and can be ecologically beneficial to downstream areas deprived of sediment for years. To employ this option, project proponents must estimate the sediment quantity to be released and, if substantial, estimate how long it will take to erode, where it will go and how long it will stay there. We investigated these issues when the Bloede Dam was removed from the Patapsco River in Maryland, USA, in 2018. The dam was about 10 m high, and its impoundment was nearly filled with an estimated 186 600 $m^3$ of sediment composed of 70% sand and 30% mud. After removal, using elevation surveys generated by traditional methods as well as structure-from-motion (SfM) photogrammetry at high temporal resolution, we documented rapid erosion of stored sediments in the first 6 months (~60%) followed by greatly reduced erosion rates for the next two and a half years. A stable channel developed in the impoundment during the rapid erosion phase. These results were predicted by a two-phased erosion response model developed from observations at sand-filled impoundments, thus expanding its applicability to include impoundments with a sand-over-mud stratigraphy. A similar two-phase erosion response has been reported for sediment releases at other dam removals in the United States, France and Japan across a range of dam and watershed scales, indicating what practitioners and communities should expect in similar settings. Downstream, repeat surveys combined with discharge and sediment gaging showed rapid transport of eroded sediments through a 5-km reach, especially during the first year when discharges were above normal, and little overbank storage.

**KEYWORDS**
channel evolution, dam removal, deposition, erosion, fluvial geomorphology

## 1 | INTRODUCTION

Dam removals have become more common in the past two decades, but they are still relatively infrequent considering the ubiquity of dams on river systems around the world (Belletti et al., 2020; Bellmore et al., 2017; Ding et al., 2019; Lehner et al., 2011; Mulligan et al., 2021). Detailed studies of river response to dam removal are rarer yet, so there is still much to learn about the physical and ecological changes in fluvial systems affected by these actions (Bellmore et al., 2017; Bellmore et al., 2019; Ding et al., 2019).

Investigations of physical responses to dam removal are the most common type of dam removal study, and available data suggest that channel recovery is often rapid—especially in former impoundments (Bellmore et al., 2017; East & Grant, 2023; Major et al., 2017). These

areas can stabilise over a period of months rather than years, frequently following a two-phase pattern first described by Pearson, Snyder and Collins (2011) and further developed by Collins et al. (2017). The first phase is rapid and characterised by the incision of stored sediments to the pre-dam channel elevation (base level) and channel widening. During this 'process-driven' phase, the increased energy gradient caused by base -level lowering is sufficient to erode as much as half of the stored sediments in a few months without large floods and sometimes with only very modest discharges (Collins et al., 2017; Major et al., 2012; Pearson, Snyder & Collins, 2011). Once a stable channel is developed in the former impoundment that is wide enough to convey the prevailing discharges of the first phase, a second, more protracted, 'event-driven' phase begins. During this time, further substantial erosion requires flood events large enough to overtop the newly formed, incised channel banks to access more distant stored sediments [generally 5-year recurrence interval floods ($Q_5$) or greater; Collins et al., 2017]. Lesser amounts of lateral erosion may occur during this phase between events, but dams are frequently built in relatively steep, confined reaches where lateral erosion is not a major process. The event-driven phase can last many years depending on a range of factors such as valley morphology, stored sediment caliber and grain size distribution, vegetation feedbacks and event magnitudes and/or frequencies.

Pearson, Snyder and Collins (2011) and Collins et al. (2017) observed the two-phase erosion response with relatively small, rapidly breached, sand-filled impoundments in the Northeast United States, but it has since been reported for removals of a range of dam sizes and stored sediment quantities in a variety of environmental settings in the United States, France and Japan—including staged removals (Bountry, Lai, & Randle, 2013; Collins et al., 2017; East et al., 2018; Gilet et al., 2021; Itsukushima et al., 2019; Major et al., 2012; Nagayama et al., 2020; Randle et al., 2015). Ferrer-Boix, Martín-Vide & Parker (2014) found similar results in a flume study of staged dam removal: much of the sediment erosion occurred soon after dam removal regardless of flow magnitude. However, not every study of physical responses to dam removal has been able to, or sought to, evaluate the two-phase model of impoundment erosion because of site conditions (e.g., minimal base-level fall; Harrison et al., 2018), data collection schedules (e.g., post-removal monitoring beginning many months after removal, likely after the rapid process-driven phase; Ibisate et al., 2016) and/or study objectives. More empirical data are therefore needed to refine the conceptual model and understand the range of conditions for which it is applicable.

To further investigate how river channels respond to dam removals that feature uncontrolled releases of stored sediment, we studied the 2018 removal of Bloede Dam on the Patapsco River, Maryland, USA, explicitly evaluating whether the two-phase model of impoundment erosion predicted the erosion response there. Based on the model, we hypothesised that approximately half of the stored sediment quantity would be eroded in less than 6 months in a process-driven phase (i.e., driven by base-level fall). The Bloede Dam removal offered the opportunity to investigate another hypothesis: that a basal mud stratum underlying the sands impounded at the site would not significantly change the two-phase pattern but may modulate erosion rates in the second phase because of the greater cohesion of these sediments when compared to the sand-filled impoundments where the model was developed. The stratigraphy of the sediments stored behind Bloede Dam has not been reported for other dam removals to our knowledge, but it may not be uncommon in narrow, riverine impoundments with relatively high dams. When the reservoir is young, the deeper, lacustrine conditions near the dam may preferentially settle fine-grained sediments as coarser material drops out in the upper reservoir. Over time, as the lower reservoir becomes shallower with sedimentation, the flow throughout the impoundment may become too energetic to settle fines and only coarse sediments will aggrade. In addition to evaluating the two-phase erosion response model, we also documented the near field, downstream channel response to the sediment release.

## 2 | METHODS

### 2.1 | Study area

The Patapsco River drains a 950-km$^2$ watershed west of Baltimore, Maryland, USA (Figure 1a). The fluvial geomorphic characteristics of the Patapsco change considerably in our study area at the Fall Line, an important regional physiographic boundary where the Piedmont meets the Atlantic Coastal Plain. Upstream of the Fall Line, the study area is gravel-bedded and flows close to bedrock in a comparatively steep, incised and confined valley (Costa, 1975; Maryland Department of Natural Resources Watershed Services [MDNRWS], 2005). Channel bed gradients in free-flowing reaches are about 0.002. Downstream in the Coastal Plain, the river is unconfined, lower gradient (0.0004) and sand-bedded (Figure 1b; Collins et al., 2017). Bordering land use also changes considerably at the Fall Line: the Piedmont section flows through the relatively undeveloped Patapsco Valley State Park, but urban development is prevalent in the Coastal Plain reaches. Suburban and urban development also surrounds the park. The Patapsco River is wadeable at average flows throughout our study area.

The Baltimore region has a humid subtropical climate (Cfa in the Köppen classification system; Beck et al., 2018). Annual precipitation at Baltimore Washington International Airport, less than 15 km from the study area, is about 1145 mm and relatively evenly distributed throughout the year (NOAA, 2023). The Patapsco River annual hydrograph is characteristic of Northeastern U.S. rivers: The highest daily median streamflows occur during the late-winter/spring runoff period and the lowest flows are in August through early October. Floods occur throughout the year, generated by a variety of mechanisms including winter–spring mid-latitude cyclones, convective rainfall and tropical cyclones (Collins, 2019; Smith et al., 2010; Smith, Villarini, & Baeck, 2011). Study site discharges are affected by storage and diversion at Liberty Reservoir (Figure 1a), a municipal water supply for the city of Baltimore completed in 1956 and two other upstream water supply diversions. Average annual discharge for water years 2011–2021 at the upstream end of the study reach at U.S. Geological Survey (USGS) gage 01589025 (Patapsco River near Catonsville, Maryland, hereafter 'Catonsville'; Figure 1c), including two very wet years in 2018 and 2019, is about 8 m$^3$/s (Winter et al., 2020). The mean annual flood for the period 1971–2021, estimated using the longer record at USGS gage 01589000 6 km upstream (Patapsco River at Hollofield, Maryland, hereafter 'Hollofield'; Figure 1a), is approximately 315 m$^3$/s.

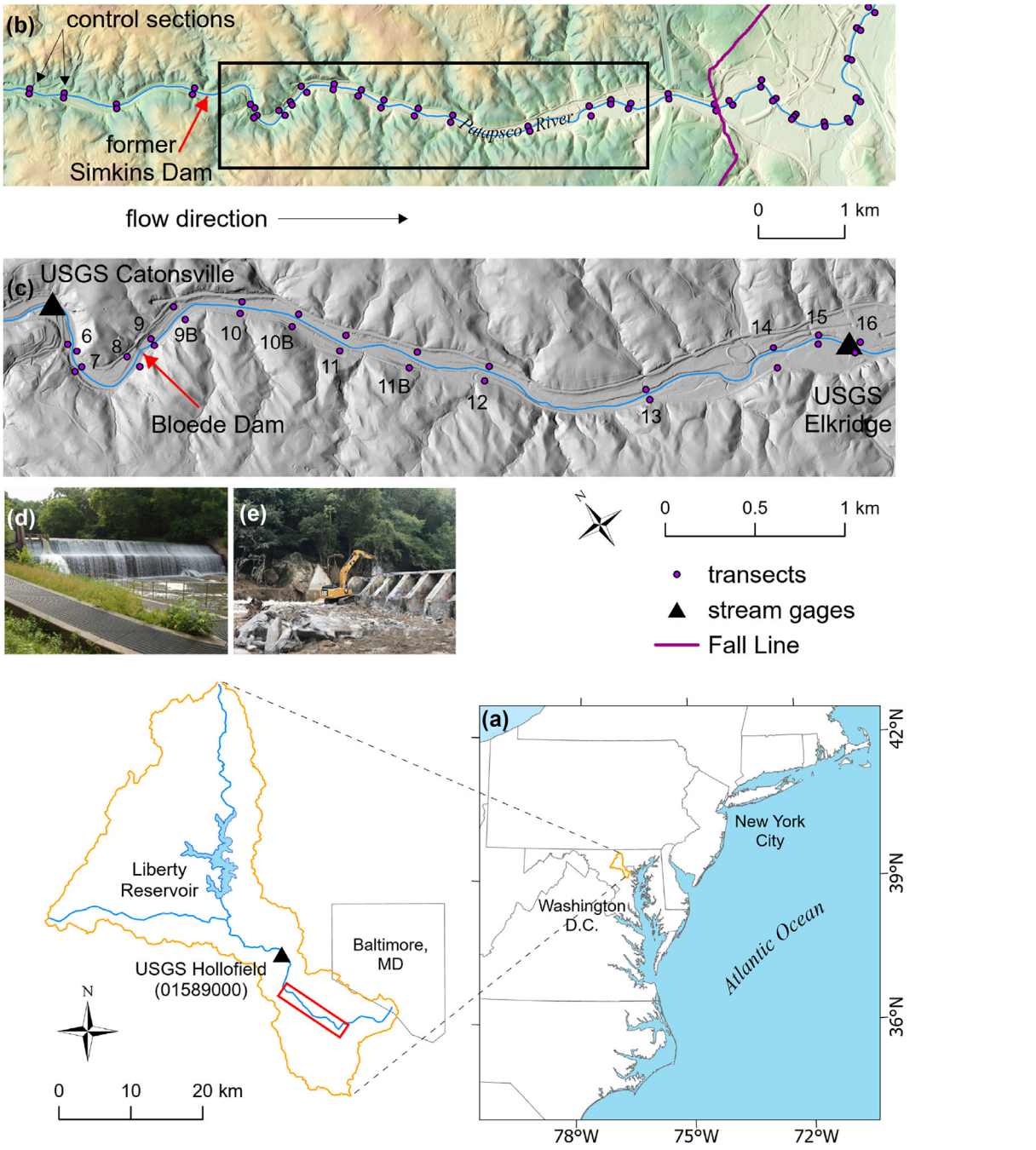


**FIGURE 1** The Patapsco River watershed in Maryland, USA (a), shaded relief of the lower Patapsco Valley (b), hillshade of the Bloede Dam removal study reach (c) and the Bloede Dam before (d) and during removal (e). County LiDAR data are available at MD iMAP (2023a).

The ~10-m-high Bloede Dam was removed from the lower Patapsco River in September 2018 to improve public safety, aquatic habitat and migratory fish passage (Figure 1c–e). Built in 1907 as a hydroelectric dam, its impoundment was filled with sediment to within 1.5 m from the dam crest within a decade and it stopped producing power in 1924 (Christianson, 2016; Synergics, Inc., 1989). The impoundment remained nearly filled with sediment at the time of removal with a shallow, riverine reservoir and a substantial area of vegetated, subaerial sedimentation. Those stored sediments, approximately 186 600 $m^3$ of sand and mud, were available for release to the downstream reach that extends about 20 river km to the Chesapeake Bay. Nearly a decade before the Bloede Dam removal, the ~3-m-high Simkins Dam less than a kilometer upstream was removed (Figure 1b). Collins et al. (2017) documented the erosion of the Simkins stored sediment, approximately 67 000 $m^3$ of sand and gravel, and its downstream transport—including temporary storage in the Bloede impoundment. Cashman et al. (2021) also used analysis of the USGS gages to provide high-resolution temporal changes associated with the arrival and dispersal of the dam removal sediment pulse downstream, including changes to local hydraulic conditions.

## 2.2 | Channel morphometry

To investigate the erosion and proximal downstream fate of the stored sediment released when Bloede Dam was removed, we used a lower Patapsco River transect network established in 2009 to study the Simkins Dam removal (Figure 1b; Collins et al., 2017). We

modified the network to reduce data collection near the former Simkins impoundment and increase data collection downstream of Bloede Dam. In the focus area for this study, shown in Figure 1c, we added transects 9B, 10B and 11B downstream of Bloede Dam. We also surveyed the Bloede Dam impoundment (from just downstream of transect 6 to the dam crest) at high spatial resolution to create digital elevation models (DEMs) and DEMs-of-difference (DoDs).

Transects were surveyed with an estimated 2 mm relative vertical accuracy using a Topcon ES-103 total station (TS; Topcon Corporation, Tokyo, Japan) and prism pole. Horizontal control in Maryland State Plane U.S. Survey Feet was established with a Topcon RTK GPS with an estimated horizontal accuracy of about 10 mm. The vertical datum was NAVD88 in feet. Tapes were extended between transect endpoint monuments and elevations were taken about every 1.5 m or more frequently to capture important geomorphic features like bank top and base, edge of water and thalweg or to delimit notable changes in bed sediment facies. We surveyed the transects twice pre-removal; the spring 2018 survey was just months beforehand (Figure 2a). They were surveyed five more times post-removal with a relatively high frequency in the first year (December 2018, March–April 2019, Jul 2019) that diminished thereafter (March 2020, March–April 2021). Our survey timing was designed to capture the rapid changes that occurred shortly after removal and/or events and was adjusted over time to reflect stabilizing conditions. An additional transect survey is shown in Figure 2a in August 2020. This covered the most downstream transects only (20–26) that are outside the study reach for this analysis. These transects were supposed to be surveyed in March 2020, but COVID-19 pandemic restrictions suspended that campaign.

We also used the TS to survey the Bloede impoundment in much greater detail to produce DEMs before removal (August 2018), a year later (August 2019) and again in August 2021 (Table 1 and Figure 2a). Cross-sections of the impoundment were surveyed approximately every 10 m in the manner done for the monumented transects, and point elevations between, or surrounding, these cross-sections were taken if they included notable geomorphic features. DEM cross-sections were staked and georeferenced for re-occupation in subsequent surveys. Above-average flows made some parts of the channel through the impoundment too deep to wade with the prism pole in August 2018, so elevation data were collected in those areas with a boat-mounted Knudsen 320B/P dual frequency echosounder (Knudsen Engineering Ltd, Ontario, Canada) with Ashtech DG-16 DGPS (Ashtech, Ohio, USA) and merged with the TS point elevations during post-processing and DEM generation.

DEMs of the impoundment topography/bathymetry were also developed at high spatial resolution from uncrewed aerial system (UAS) imagery and structure-from-motion photogrammetry (SfM). This approach was especially useful for documenting channel and valley change during, and shortly after, the removal when the area was not surveyable with the TS (Figure 2a). Imagery for SfM DEMs included in this analysis was collected on 13 September 2018, 23 October 2018, 28 February 2019 and 30 January 2020 (Table 1 and Figure 2a).

UAS imagery was collected by a DJI Phantom 4 Pro quadcopter (succeeded by the Mavik 2 model; DJI, California, USA) with preprogrammed flight paths at a consistent altitude of 350 ft (~100 m) above the channel and pre-set image overlaps of 90%. Images were

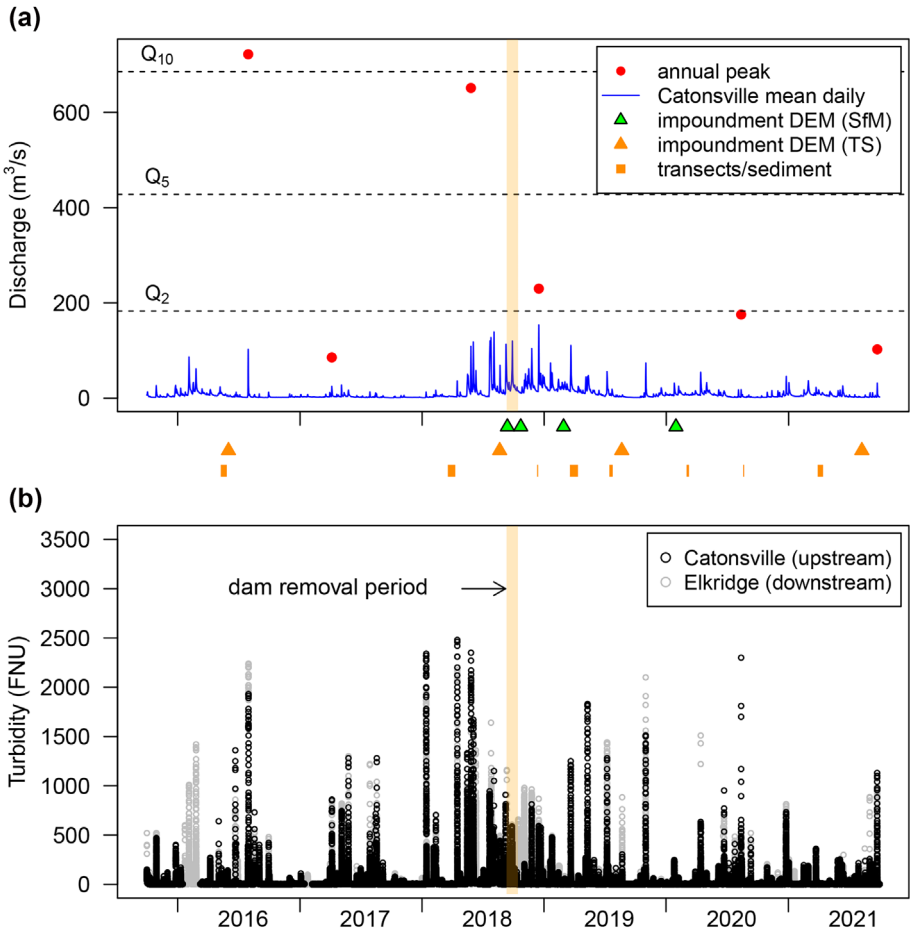


**FIGURE 2** (a) The Patapsco River hydrograph immediately upstream of the dams (Catonsville) during the study period and the timing of digital elevation model (DEM), transect and bed-sediment surveys. Rectangle widths indicate transect/sediment survey durations. Horizontal dashed lines show the estimated magnitudes of 2-, 5- and 10-year floods based on Log-Pearson Type-III analyses of annual instantaneous peak flows from 1971 to 2021 at Hollofield. (b) The turbidity time series upstream and downstream of the dam. SfM, structure-from-motion; TS, total station.

**TABLE 1** Bloede impoundment erosion quantities and rates.

| Survey | Days since breach | Erosion quantity (t) | Upstream remaining[a,b] (t) | (%) | Erosion rate (t/day) |
|---|---|---|---|---|---|
| 11 September 2018 | 0 | 0 | 246 000 | 100 | 0 |
| 13 September 2018 | 2 | −16 000 ± 10 000 | 231 000 | 94 | 8000 |
| 23 October 2018 | 42 | −65 000 ± 15 000 | 166 000 | 67 | 2000 |
| 28 February 2019 | 170 | −66 000 ± 15 000 | 100 000 | 41 | 400 |
| 21 August 2019 | 344 | 8000 ± 10 000 | 107 000 | 44 | −20 |
| 30 January 2020 | 506 | −5000 ± 9000 | 103 000 | 42 | 10 |
| 08 August 2021 | 1062 | 5000 ± 9000 | 108 000 | 44 | −10 |

[a]Mass estimate at day 0 based on our estimate of 186 600 $m^3$ of stored sediment in August 2018 and a bulk density of 1.32 $t/m^3$.
[b]Cumulative storages in tonnes were calculated retaining at least one additional significant figure than reported; thus, values down column cannot be reproduced exactly by subtracting the erosion quantities in the adjacent column from the initial stored sediment quantity of 246 000 t. The estimated upstream remaining quantity of 108 000 t by August 2021 is ±68 000 t (error accumulated from the adjacent column). We believe this cumulative error estimate is conservative because a direct differencing of our August 2018 and August 2021 total station digital elevation models (TS DEMs; not shown) yields a similar estimate of the quantity remaining upstream, but the estimated error is only 1/3 as large.

collected at the nadir and 30 degrees off the nadir to capture views underneath overhanging vegetation along channel banks. Images were processed via Agisoft PhotoScan (AgiSoft PhotoScan Professional [Version 1.2.6] [Software], 2016) to develop orthoimages of the impoundment for each flight date, and associated DEMs, generally following an SfM workflow described by Woodget et al. (2015). DEMs were compared to surveyed ground control points and assessed for evidence of internal error using methods described by James et al. (2017). SfM DEMs produced via these methods were also validated by comparing their outputs with contemporaneous TS cross-section measurements for dates and stream reaches when both methods were employed (e.g., March 2018 and April 2021; the impoundment was never surveyed at the same time by both methods). Errors were estimated as root mean square errors (RMSEs) with TS elevations assumed to be the true elevations. Based on these comparisons, we estimate vertical errors in our SfM DEMs to be between 0.15 and 0.3 m. Average subaqueous RMSE values were sometimes higher than average subaerial RMSEs (0.26 and 0.23 m, respectively) and respective mean absolute errors indicated bias consistent with refraction in wetted areas of the channel. These SfM vertical error estimates include errors associated with point-to-raster interpolations necessary to generate a DEM surface; thus, they are not directly comparable to vertical accuracies reported above for TS vertical measurements. Errors associated with point-to-raster interpolations for the TS DEMs are included in the uncertainty estimate reported below for DEM differencing—see '*Estimating impoundment erosion quantities and rates and associated uncertainty*'.

## 2.3 | Sediment sampling

We evaluated bed sediment grain size distribution while we surveyed monumented transects, assessing areas extending about 7.5 m upstream and downstream of each. We would first visually identify and field map discrete areas of relatively homogeneous sediment texture (i.e., facies) and then sample each. For infrequent instances when we encountered relatively deep water with poorer visibility, facies were confirmed with a clamshell sampler deployed from a small boat or by probing the bottom with a survey pole. Coarse-grained facies dominated by clasts larger than granules ($D_{50} = 6$ mm), determined visually, were sampled via Wolman pebble counts (minimum 150) to quantify the grain size distribution. Pebble counts were conducted in water depths generally less than 0.3 m. Finer facies (i.e., sand and finer) were bulk sampled to a depth of about 0.3 m below the bed and then sieved in the laboratory. Samples for the laboratory containing primarily coarser material (sands and some gravel) were dry sieved only through a series of 10 sieves ranging from 75 μm to 16 mm. Sediments that passed through the 75 μm sieve were classified as silts. Samples with a higher proportion of silts and clays were first wet-sieved through a 0.0625-mm mesh sieve (U.S. Standard Sieve #230). The gravel sand fraction retained was then dried, weighed and saved for further sieving at whole phi intervals with the largest sieve having a 4-mm mesh. The finer silt and clay-sized particles passing the #230 sieve were then separated and graded via the pipette method (Van Ryswick et al., 2017).

Most facies were sampled at least once during each field campaign. The grain size distributions of facies with multiple samples were averaged and used to represent the texture of those facies at transects where they were not sampled during the same campaign. There were instances when a facies was mapped during a campaign but not sampled at that time. In those infrequent cases, we averaged the grain size distributions for all campaigns when the facies were sampled. The facies maps for each campaign were digitally rendered in a geographic information system, the per cent of the transect area occupied by each facies was computed, and the $D_{50}$ for the facies with the greatest area was used to represent the transect texture for that period.

Cores taken for pre-removal engineering studies indicated that the stored sediments were primarily sands and the lower impoundment had a mud stratum at the base. To estimate the dry bulk density of the mud stratum, we took two samples from post-removal exposures along the left bank: one behind the dam near the location of core b1 and another upstream close to where the unit pinches out (near core b17; Figure 3). We also took a bulk density sample of the overlying sands at an exposure along the left bank near core b5. At each sample location, we took three subsamples of the target stratum by digging back to develop a fresh exposure, driving a plug of known volume flush with the surface (~50 $cm^3$) and carefully extracting the

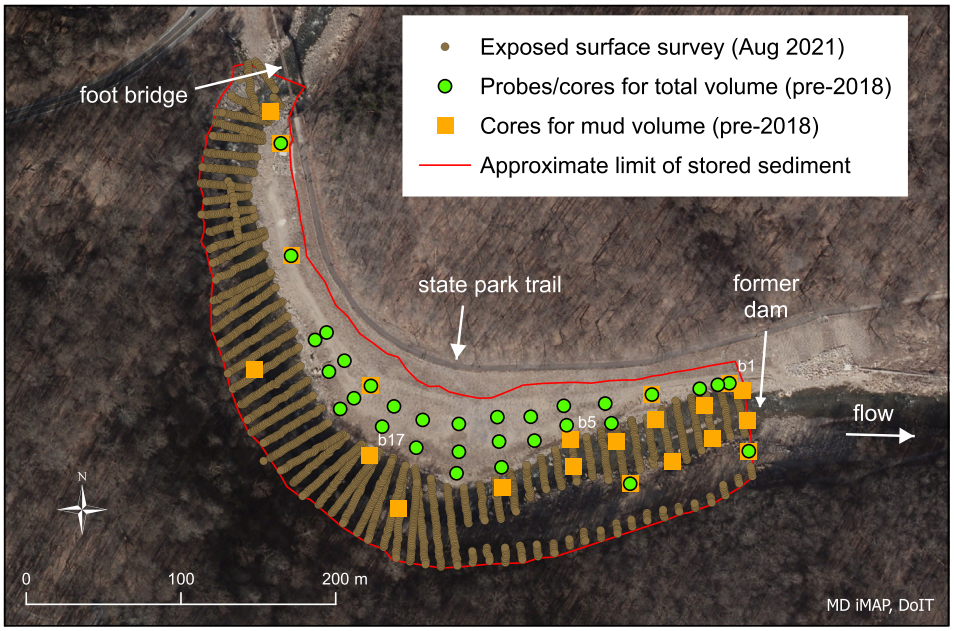


**FIGURE 3** Exhumed pre-dam surfaces surveyed in August 2021 (small, tan circles) and 31 cores (larger, light green circles) used to determine pre-dam elevations beneath remaining stored sediment. Seven of these cores (light green circles over orange squares) had detailed stratigraphic descriptions that were used to estimate the sand and mud-sized fractions of the stored sediment along with another 14 cores with detailed stratigraphy (orange squares). The three labelled cores are at the approximate locations of dry bulk density samples taken post-removal. The aerial image was taken in 2020 (MD iMAP, 2023b).

plug to avoid sediment loss. Each subsample was then placed into an airtight bag and labelled for transport to the laboratory where they were dried and weighed using a scale with 0.001-g precision. The dry mass of the subsample was then divided by its volume to determine the dry bulk density ($\rho_{dry}$). We also determined the grain size distribution of each subsample using the method described above for the streambed sediment samples. The respective values for the three subsamples at each location were then averaged to estimate the dry bulk density and grain size distribution for that sample.

Four bulk density samples taken from the Simkins impoundment upstream shortly after the Simkins dam removal were used in conjunction with the post-removal sample of the overlying sands in the Bloede impoundment (described above) to estimate the bulk density of the Patapsco River sands (Collins et al., 2017).

## 2.4 | Discharge and turbidity gaging

Site hydrology provides context for our morphometric analyses. We used the 10-year record at the Catonsville gage for average daily discharge. For flood hydrology, we used the longer record of annual instantaneous peaks 6 km upstream at Hollofield, adjusting for a 6% increase in drainage area. We suspect that this drainage–area correction may underestimate flood magnitudes at the dam removal site because the upstream watershed at Hollofield is influenced by Liberty Reservoir and largely rural land cover while the contributing areas downstream to Catonsville have more urban influence. We chose the 1971–2021 period to represent the modern flood regime and a consistent influence of upstream storage and diversions (Armstrong, Collins, & Snyder, 2014). Floods of specified annual exceedance probabilities and associated recurrence intervals were estimated using methods described by England et al. (2019) and implemented via PeakFQ 7.4 with the expected moments algorithm (Veilleux et al., 2014). We used the 15-min streamflow record downstream of the dam at USGS gage 01589035 (Patapsco River near Elkridge, Maryland, hereafter 'Elkridge'; Figure 1c) for a limited analysis of potential changes in bed elevation at that section using the specific discharge methods of Cashman et al. (2021). A specific discharge analysis evaluates changes through time in the discharge needed to attain a given water surface elevation (i.e., stage) due to changes in channel geometry and/or hydraulics.

Turbidity was measured every 15 min upstream at Catonsville and downstream at Elkridge using Forest Technology Systems DTS-12 turbidity sensors. The sensors report formazin nephelometric units (FNU) with a dynamic range between 0 and 1600 FNU. Turbidity data were collected, quality assured/quality controlled and approved following standard USGS protocols outlined in Wagner et al. (2006). All discharge, stage and field measurement data were collected, quality assured/quality controlled and approved according to standard USGS surface water protocols outlined in Turnipseed and Sauer (2010) and Sauer (2001). Discharge and turbidity data are publicly available for each site on the USGS National Water Information System (U.S. Geological Survey (USGS), 2023) (https://doi.org/10.5066/F7P55KJN).

## 2.5 | Estimating impoundment erosion quantities and rates and associated uncertainty

To estimate the quantity of sediment stored behind Bloede Dam at the time of removal in Sep 2018, we first had to estimate the elevations of the pre-dam valley, create a DEM from those elevations and then subtract that DEM from a DEM of the impoundment surface surveyed in August 2018. Pre-dam valley elevations were established by combining post-removal surveys of exhumed pre-dam surfaces and, for areas where stored sediment remained, estimates from 24 probes to refusal and seven stratigraphic cores taken for dam removal planning studies (Figure 3). The seven cores, and 14 other stratigraphic cores not used for the quantity estimate because they were extracted from locations where the pre-dam surface was exhumed and thus surveyable, also enabled us to estimate the grain size composition of the stored sediment. Mud-sized sediment facies, if they were encountered, were always underlying coarser facies and were aggregated toward the left side of the impoundment. This enabled us to create a DEM of the top of the mud unit from which we subtracted the

elevation of the pre-dam valley surface to estimate the total volume of mud and its proportion of the total stored sediment volume.

We differenced DEMs to estimate the erosion quantities and rates in the Bloede impoundment for time periods between post-removal TS or SfM surveys. To avoid spurious elevation changes when differencing TS and SfM DEMs, we used a polygon common to successive DEMs that excluded areas with overhanging trees where the SfM surveys did not accurately capture ground surface elevations. Excluding these areas, primarily along the right bank, had negligible effects on our computations because areas under trees showed little to no erosion or deposition over the project period in our TS surveys. Our differencing polygons also excluded areas of stored sediment on the left bank that were subject to earth moving for dam removal and associated construction activities. This too had little impact on our estimates because fluvial erosion and deposition were not active in these areas, no sediments trapped by the dam were mechanically removed from the site and no sediments were trucked to the area from off-site. Evidence that excluding these areas had little effect on our DoD results is the fact that our cumulative erosion estimate for the August 2018 to August 2021 study period by differencing all successive TS/SfM surveys with the smaller polygon is within 5500 $m^3$ of the erosion estimated for the same interval by differencing only the TS surveys with the full polygon. This is less than the estimated uncertainty of a TS/SfM DoD for a single survey interval (see below).

We used RMSE as a measure of uncertainty for our DoDs and estimated it by differencing TS and SfM DEMs bracketing a period when elevation changes should have been zero. Doing so includes random and systematic measurement errors associated with field measurements, post-processing (including point-to-DEM surface interpolation errors), and employing two DEM generation methods. We chose the 5-month period between 21 August 2019 (TS) and 30 January 2020 (SfM) because there were no overbank flows during this time and contemporaneous transect measurements at XS7 and XS8 showed virtually no change over a bracketing interval (July 2019 to March 2020; Figures 1 and 2a). DoD uncertainty based on this approach, as a 95% confidence estimate (i.e., 1.96*RMSE), is 6815 $m^3$, or approximately 0.2-m elevation over the impoundment area that has eroded.

We ultimately evaluated our erosion quantities and rates as masses rather than volumes, so we also estimated the uncertainty of our bulk density estimate and propagated both uncertainty sources as ordinary sums rather than in quadrature because they include systematic and random uncertainties (Taylor, 1997). The uncertainty of the mean bulk density, 9.1%, was estimated by the standard error (SE) of the seven measurements used to compute it at 95% confidence (1.96*SE).

## 3 | RESULTS

### 3.1 | Stored sediment quantity

We estimated there was about 186 600 $m^3$ of stored sediment behind Bloede Dam just before removal that was composed of 70% sand and 30% mud. The sediment cores indicated that the mud facies occurred at the base of the stored sediment primarily along the left side of the impoundment and that the thickest accretions were in the lower half near the dam (Figure 4). This matched the stratigraphy we observed soon after dam removal as the sediment deposit was rapidly incised and evacuated. We also observed some thin, discontinuous layers of decomposing organics in the deposit.

The dry bulk densities of our two samples from the basal mud stratum were each 1.22 t/$m^3$, within the range of our lower Patapsco River sand samples (1.07–1.53 t/$m^3$). This likely reflected the relatively high sand content and poor sorting of each mud sample. Indeed, the farthest upriver sample, near where the mud pinched out, was slightly dominated by sand (52% and thus not truly mud). The mud sample from the lower reservoir also had a relatively high sand content (38%), which aligns with descriptions of the mud when it was encountered in the pre-removal cores. In the driller's logs, it is frequently described as having small amounts of sand. The overlying sands are often described as having smaller fractions of silt and/or clay.

Given the dry bulk densities of the mud stratum are within the range of those for the sand samples, there is no justification for discretizing the mass of the stored sediment quantity by stratigraphy (at the resolution it has been described and sampled at the site). Therefore, to estimate the mass of the stored sediments we used an average dry bulk density value computed from our five sand samples (1.07, 1.29, 1.43, 1.46 and 1.53 t/$m^3$) and two mud samples. Two approaches, an arithmetic average of the seven samples and an average of the sand and mud samples weighted by their volumetric proportions (0.7 and 0.3, respectively), produced the same estimate of 1.32 t/$m^3$.

### 3.2 | Impoundment erosion quantities and rates

Figure 5 shows a DoD of the Bloede impoundment comparing the pre-removal surface (August 2018) with the surface at the end of our study period (August 2021). The lower impoundment has as much as 9.5 m of vertical erosion to the pre-dam bed elevation. Table 1 and Figure 6 show how these sediments were rapidly eroded in the first 6 months after removal (~60%) during a period of elevated daily discharges but no flows greater than a 5-year recurrence interval flood ($Q_5$). Flood events greater than $Q_5$ are generally larger than channel forming, or effective, discharges and frequently go overbank (Wolman & Miller, 1960). There was virtually no erosion for the next two and a half years (the three surveys after February 2019 show small erosion or deposition quantities that are within measurement error). A vertically and laterally stable channel flowing on the pre-dam surface was developed through the impoundment during the rapid erosion phase. Figure 7 shows how the bed sediment texture in the impoundment dramatically coarsened during this time to a texture similar to that found upstream and downstream. Indeed, the dominant bed sediment texture in the former impoundment today is coarser than nearby reaches, which aligns with this reach being the steepest in the study area (Figure 7).

### 3.3 | Downstream fate

Downstream, eroded sediments moved relatively rapidly through the study reach with only a few transects showing persistent, but modest,


**FIGURE 4** Mud thickness contours showing the greatest accretions near the left bank and in the lower half of the former impoundment. The aerial image was taken in 2014 (MD iMAP, 2023c).

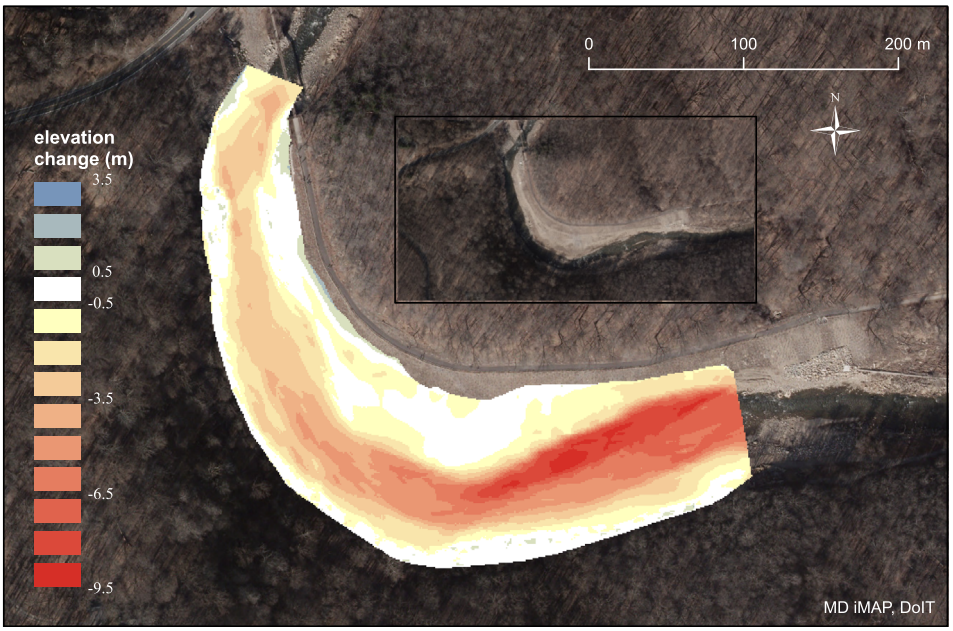


**FIGURE 5** Digital elevation model-of-difference (DoD) of the Bloede impoundment for the period August 2018 (pre-removal) to August 2021. The aerial image was taken in 2020 (MD iMAP, 2023b).

accumulations on the bed or bars. Figure 8 shows representative transects for the reach and Figures S1, S2, S3, S4, S5, S6, S7, S8 and S9 in the Supporting Information have animations of the surveys through time for nine downstream study reach transects with complete survey records (two sections were not surveyable on some survey dates). We also found no evidence for appreciable overbank deposition during the post-removal period at these sections, spaced an average of about 450 m apart, which is not surprising given there were few high flow events capable of exceeding the bank heights (Figure 6a).

Bed sediment textures at the transects in the first two kilometers downstream of the dam show how sand-sized and finer sediments moved so rapidly through this reach that little to no fining of the dominant facies is evident in the first post-removal survey in Dec 2018 (~3 months after removal) or subsequent surveys (Figure 7, Transects 9–11B). Starting at 2 km below Bloede dam and further downstream; however, we start to see a pattern where the early post-removal surveys show finer dominant facies than the pre-removal survey at a given transect. Yet, these sediments also move through relatively quickly and the most recent surveys in this reach tend to show the dominant facies have returned to a texture similar to, or coarser than, the texture found in the pre-removal survey.

Mud-sized sediments carried in suspension were detected rapidly at the downstream gage (Elkridge). Figure 2b shows a relatively brief period of elevated turbidity (~6 weeks) at Elkridge that did not occur upstream at Catonsville. Thereafter, however, upstream and downstream turbidity looks similar with the exception of a few events in the latter half of 2019 and early 2020 when the downstream spikes had moderately greater magnitude and likely indicate some episodic erosion of mud in the impoundment.

## 4 | DISCUSSION

The Bloede Dam removal provided an excellent opportunity to evaluate the two-phase erosion response model of Pearson, Snyder and Collins (2011) and Collins et al. (2017). From their model, we

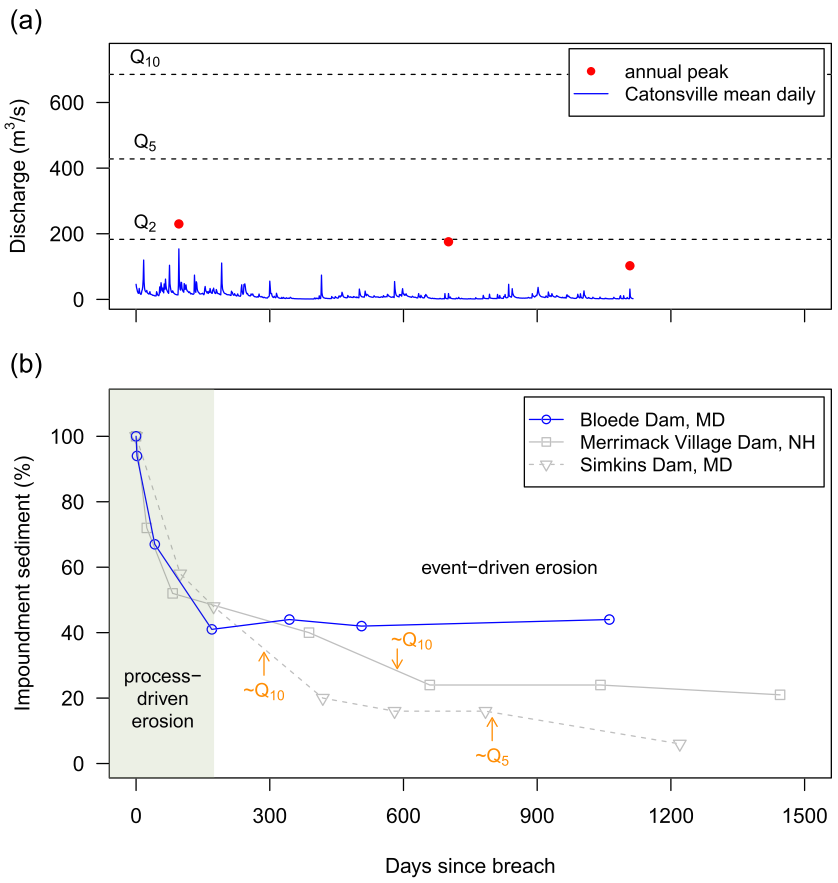


**FIGURE 6** (a) Patapsco River mean daily and annual peak flows at Catonsville during the post-removal period and the estimated magnitudes of 2-, 5- and 10-year floods. (b) Bloede impoundment erosion quantities and rates expressed as a percentage of the total stored sediment quantity remaining at successive time horizons since the breach date (Table 1). Also shown are erosion quantities and rates for the Simkins Dam (removed upstream in 2010) and the Merrimack Village Dam (removed from the Souhegan River, New Hampshire, USA, in 2008) and the relative timing of post-removal floods larger than Q5 at those sites (Collins et al., 2017).

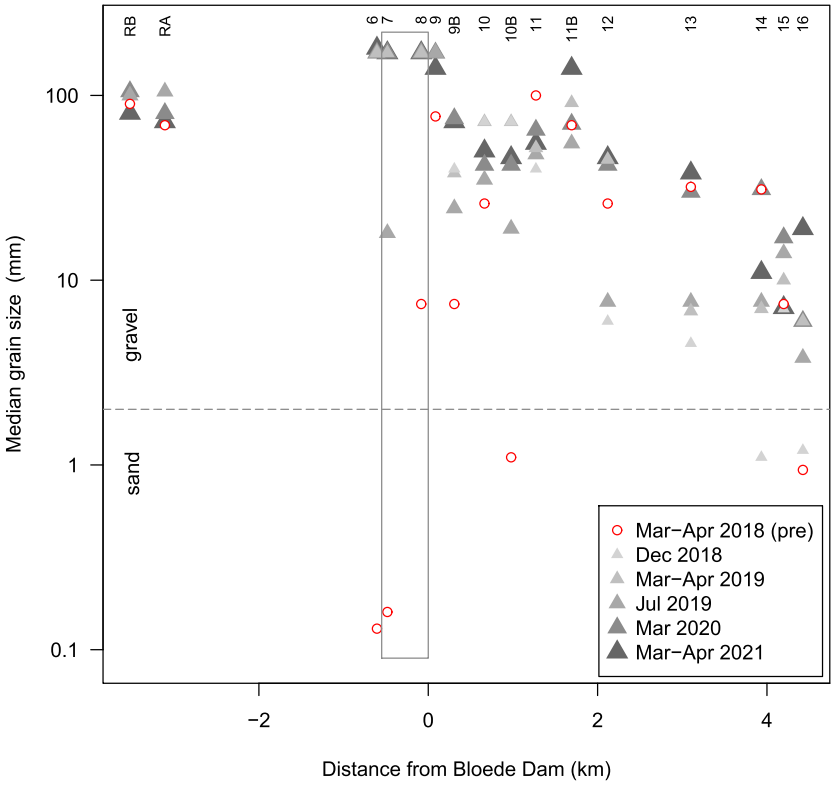


**FIGURE 7** Changes through time in the median grain size ($D_{50}$) of the dominant bed sediment facies at each study reach transect and the control sections upstream (see Figure 1b). The grey rectangle shows the spatial extent of the Bloede impoundment. Note that March–April 2018 (pre) values in the impoundment are for the surface of the stored sediments.

developed two testable hypotheses for the Bloede site: (1) approximately half of the stored sediment would be eroded in less than 6 months in a process-driven phase (i.e., driven by base-level fall) and (2) a basal mud stratum would not significantly change the two-phase pattern but may modulate erosion rates in the second phase because of the cohesion of the mud forming the banks of the channel through the lower impoundment. Here, we discuss our results in the context of these hypotheses, but we begin with some information and

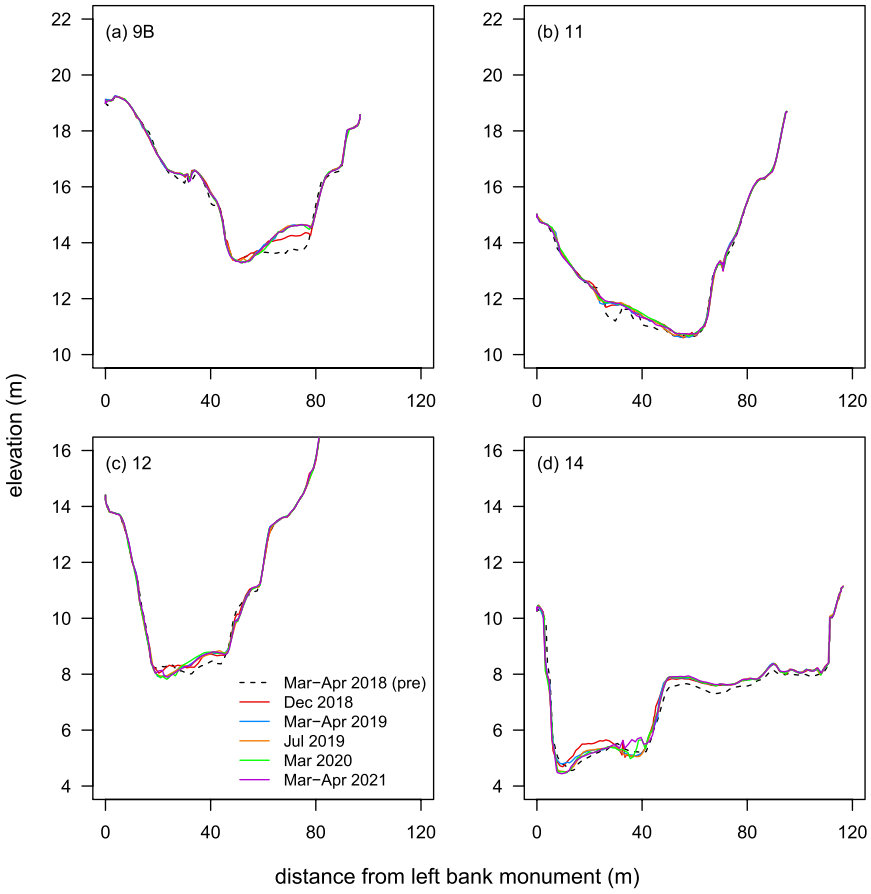


**FIGURE 8** Example transect elevation changes downstream of the Bloede impoundment. Transect locations are shown in Figure 1c at these distances downstream of the former dam: 0.3 km (9B), 1.3 km (11), 2.1 km (12) and 3.9 km (14). Vertical datum is NAVD88.

observations related to our stored sediment quantity estimate that have particular relevance for dam removal practitioners. Our data on the downstream fate of the released sediments are also discussed.

## 4.1 | Stored sediment quantity

Our estimate that the stored sediment was about 70% sand and 30% mud generally matches the proportions estimated during pre-removal engineering studies for the project, but our total stored sediment estimate (186 600 $m^3$) was about 20% less. The difference between estimates reflects a real change in stored sediment quantity between 2018 and 2012 when the engineering studies were completed, additional data available to us after removal (i.e., exhumed pre-dam surfaces) and different methods.

The sediment quantity behind Bloede Dam changed in this 6-year period for several reasons. First, in 2011 and 2012, the reach between the USGS Catonsville gage and transect 6 was still aggraded with sandy sediments released during the Simkins Dam removal (Figure 1c). These were included in the engineer's estimate of sediments available for release by the Bloede Dam removal because it was unclear how long these sediments would remain there or in the impoundment below. Later studies showed that a substantial amount of these sediments was eroded from the reach by Nov 2013 and carried further downstream (Collins et al., 2017). Second, large floods in July 2016 and May 2018, estimated to be about 10-year recurrence interval events, potentially caused net erosion in the Bloede impoundment. Sediments stored behind run-of-river dams can be episodically mobilised during events and transported downstream when the dam is in place, especially when the impoundment is nearly filled (Pearson & Pizzuto, 2015; Pearson, Snyder, & Collins, 2011). The impoundment can then refill slowly during moderate flows or rapidly with subsequent events.

Accurate estimates of stored sediment quantities are essential for pre-removal planning and risk assessments and for scientific evaluations of post-removal system responses. However, they are challenging to achieve because of the dynamism of the deposits, exemplified at the Bloede site, and because they often require interpolation from spatially distributed cores/probes and/or other assumptions. Dam removal practitioners can best address these challenges by performing robust pre-removal sediment characterisation studies and assuring that sediment management plans are based on recent estimates of the stored sediment quantity. In the Bloede case, the stored sediment quantity decreased over the elapsed time (6–7 years) between planning and implementation, and thus, the pre-project estimates and associated risk assessments were conservative and protective. However, if quantities increase over time instead, dated estimates may be underestimates and not protective enough of downstream environmental and/or human community interests.

## 4.2 | Impoundment erosion quantities and rates

The Bloede impoundment erosion response was indeed predicted by the two-phase erosion response model developed from observations of the Simkins Dam removal upstream and the Merrimack Village Dam (MVD) in New Hampshire, USA (Collins et al., 2017; Pearson, Snyder, & Collins, 2011). While these two sites had similar dam and

watershed sizes, stored sediment quantities and grain size distributions, the two-phase erosion response has also been reported for dam removals across a range of dam and watershed scales in a variety of environmental conditions in the United States, France and Japan (e.g., East et al., 2018; Gilet et al., 2021; Itsukushima et al., 2019; Nagayama et al., 2020). For example, the model well described the erosion response for the Elwha Dam removals, which featured a sediment yield comparable in magnitude to a moderate volcanic eruption like Mount St. Helens in 1980 (East et al., 2018). During the first, 'process-driven' phase of the model, erosion is driven by the increased energy provided by base-level fall, and flow magnitude is much less important. Once a stable channel is formed in the impoundment and sediment proximal to it is eroded, larger, overbank discharges are required to access stored sediments that are more distant from the newly formed channel. Erosion during this phase is 'event-driven'.

We hypothesised that approximately half of the stored sediment at Bloede Dam would be eroded in less than 6 months after removal driven by base-level fall. Figure 6b confirms that and shows that the erosion trajectory during the process-driven phase is similar to that of the two dam removal sites where the two-phase response was first identified and described. None of the three sites had a discharge greater than $Q_5$ during this time (Figure 6; Collins et al., 2017). Significant erosion during the event-driven phases at the Simkins and MVD sites occurred only with relatively large, overbank floods with recurrence intervals ranging from 5 to 10 years (Figure 6b; Collins et al., 2017; Pearson, Snyder, & Collins, 2011). There has been no erosion during the event-driven phase at the Bloede site largely because, as of 2021, there have been no large floods (Figure 6a).

Experience at the MVD site indicates that the event-driven phase can be protracted (Figure 6b). Morphometry studies there continue nearly 15 years after removal and the quantity of stored sediment remaining in the impoundment remains around 20% (Collins et al., 2017; Noah Snyder, personal communication). In contrast, very little of the Simkins Dam stored sediment remains in its former impoundment. Collins et al. (2017) attributed the difference between the two sites in this respect to the considerably wider valley at MVD, since the sites are similar in many other respects and had a similar flood history post-removal. Wider valleys can store impoundment sediment farther from reestablished channels and thus require larger events, or sufficient time for lateral migration, to reach and mobilise them. The valley widths of the Simkins and Bloede sites are more comparable given their proximity to the same river, yet we might expect a protracted event-driven phase at the Bloede site given the different flood history in the early post-removal period and associated negative feedback with vegetation. The absence of large floods has contributed to vigorous vegetation growth on remaining stored sediments, increasing their stability. Also, the Bloede Dam was about 7 m higher than the Simkins Dam, and thus, the stored sediment surfaces are also higher; because they are distributed over the inner bend of a valley meander, very large floods will likely be necessary to access them.

We also hypothesised that the basal mud stratum at the site would not significantly change the two-phase pattern but may modulate erosion rates in the second phase. Our erosion data do not indicate that the stratigraphy of the Bloede deposit significantly changed the two-phase response from the general pattern observed at the Simkins and MVD sites where there were no mud strata (Figure 6b). Nor was a similar two-phase erosion response obscured at the Elwha dam removal sites where stored sediments had a substantial mud fraction (East et al., 2018). Our field observations also did not indicate preferential erosion of the sand or mud to the extent that the remaining sediment has substantially different proportions of each than the pre-removal deposit. Nonetheless, as we hypothesised, there is evidence that the basal mud stratum at Bloede may have contributed to the notably flat erosion curve in the event-driven phase there (Figure 6b). The greater cohesion and water retention properties of mud, compared with sand, enabled the rapid formation of stable banks conducive to the quick establishment of vegetation that was observed. Well-vegetated, cohesive banks resisted even small amounts of lateral erosion that might have been expected without events—erosion that is evident at the MVD and Simkins sites in the event-driven phase between events.

### 4.3 | Downstream fate

Pearson, Snyder and Collins (2011) noted how sand moves as bedload even during modest flows, which explains how the large release of sand to the downstream reach at the MVD site was remobilised relatively quickly despite its low gradient and periodic backwatering from floods where it joins a much larger river. Similarly, during the previous Simkins Dam removal in the Patapsco River, most channel change and transport of the sediment pulse occurred at relatively lower flows and were not closely tied to suspended sediment loading events (Cashman et al., 2021). Considering that, conditions were favorable for the rapid transit of Bloede sand observed through the downstream part of our study reach (transects 9–16; Figures 1c, 7 and 8). This is a relatively steep reach before the Patapsco enters the Coastal Plain and average daily discharges—but not floods—were unusually high for nearly a year after the September 2018 removal (Figure 2a; Winter et al., 2020). Pre-removal numerical modelling of sediment transport predicted that any substantial bed aggradation in this reach would move through within about 4–6 months under a wet period scenario and that generally matches what we observed at the cross-sections (Stillwater Sciences, 2014; Figure 8). A specific discharge analysis for the Elkridge gage, which evaluates variation through time in the discharge needed to achieve a given stage due to changes in channel geometry and/or hydraulics (sensu Cashman et al., 2021), also corroborates this. Figure 9 shows how the discharge required to attain the site's National Weather Service (NWS)-designated 'action' stage dropped during and after the dam removal, likely indicating increased bed elevation, but recovered by spring or summer of 2019 to pre-removal levels. The action stage is the lowest warning level when the river is approaching flood stage and interested parties should prepare for potential impacts (National Weather Service, 2023). The discharge needed to attain a 'minor' flood stage also dropped during this time. Specific discharge for the NWS action stage actually decreased a couple of months before the dam removal began (Figure 9). We think this may be associated with deposition from a large flood in May 2018 when nearby floodplain surfaces had evident sand and mud accretion (Figure 2a). However, a more detailed investigation of the relative influence of dam removal and large floods on bed elevation changes at the site is beyond the scope of this study and could be the subject of future work.

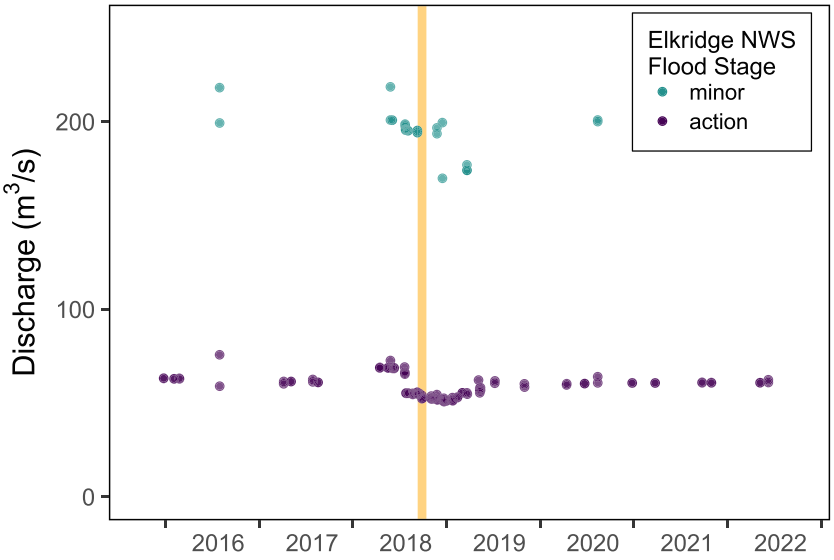


**FIGURE 9** Changes over time in the discharge needed to attain the two lowest National Weather Service (NWS)-designated flood stages at the Elkridge gage, indicative of changes in bed elevation (National Weather Service, 2023). The vertical bar shows the dam removal period.

Stillwater Sciences (2014) also predicted 4 weeks of elevated suspended sediment concentration after removal for the wet period scenario, but turbidity measurements suggest that occurred for about 50% longer (Figure 2b). The sizeable mud fraction of the stored sediment was likely a major contributor, but the mud would not be expected to deposit on the bed of the study reach during within-bank flows, consistent with our observations of minimal cross-section change (Figure 8 and S1–S9). During this relatively brief period of elevated turbidity at Elkridge, and thereafter through 2021, turbidity magnitudes never exceeded what the watershed is capable of producing during floods, as measured at the upstream gage (Catonsville; Figure 2b). This matches the findings of Tullos et al. (2016) who reported that turbidity magnitudes associated with dam removals rarely exceed those of watershed flood events.

## 5 | CONCLUSIONS

Our investigation of erosion rates at the Bloede impoundment provides additional support for the two-phase erosion response model first proposed by Pearson, Snyder and Collins (2011) for dam removal sites and further refined by Collins et al. (2017). A sand-over-mud stratigraphy did not fundamentally alter the two-phase response: Over half of the stored sediment eroded rapidly over a period of months via incision to base level (Phase 1) and further significant erosion will depend on large floods (Phase 2), which were absent during the post-removal period we observed. Our Bloede studies indicate, however, that a basal mud stratum at a dam removal site may slow erosion rates in the second, event-driven phase by accelerating dense vegetation growth on the banks and arresting even small amounts of erosion expected between events during this period.

The two-phase erosion response model can help practitioners and communities understand what to expect from similar projects and has some relevance for other situations when large quantities of sediment are rapidly delivered to stream channels—like landslides and volcanic eruptions (e.g., Gran, Montgomery, & Halbur, 2011; Major et al., 2019). However, more case studies are needed to test and potentially refine it over a broader range of geographic settings, hydroclimatic environments, dam and watershed sizes and stored sediment conditions.

Taken together with our observations of the rapid movement of eroded sediments through the downstream part of the study reach, and short-lived turbidity spikes never exceeding turbidities produced by watershed storm events, the Bloede site provides another example of how rivers can physically stabilise relatively quickly after dam removals (Foley et al., 2017). Our results may be good news for communities seeking to address concerns presented by aging infrastructure in river environments, including ecosystem impacts (Doyle et al., 2008; Graf, 2006; Petts, 1984).

## AUTHOR CONTRIBUTIONS

**Mathias Collins:** conceptualisation, methodology, investigation, resources, supervision, writing—initial draft and writing—reviewing and editing. **Matthew Baker:** conceptualisation, funding acquisition, methodology, investigation, resources, supervision and writing—reviewing and editing. **Matthew Cashman:** conceptualisation, methodology, investigation, resources, software and writing—reviewing and editing. **Andrew Miller:** conceptualisation, funding acquisition, methodology, investigation, resources, supervision and writing—reviewing and editing. **Stephen Van Ryswick:** funding acquisition, investigation, resources, supervision and writing—reviewing and editing.

## ACKNOWLEDGEMENTS

This work was supported by NOAA through Coastal and Marine Habitat Restoration Award Numbers NA13NMF4630127, NA16NMF4630317 and NA19NMF4630270 and the U.S. Fish and Wildlife Service through award F18AC00022. Eric Boyd, Brett McFarland and Ashley Ryan assisted with discharge and sediment measurements at the U.S. Geological Survey gaging stations. Chris Connallon, Anna Gillmor, Bryan Nicholson and Beth Sylvia with the Maryland Geological Survey collected and processed topographic, bathymetric and facies measurements. Jack Hardway, Kristian Nelson, Alex Rittle and Ryan Wooldridge collected and processed aerial imagery for SfM DEMs. Feedback from Tim Beechie, Jennifer Bountry, Andrew Wilcox and an anonymous reviewer improved an earlier

version of the manuscript. Any use of trade, firm or product names is for descriptive purposes only and does not imply endorsement by the U.S. Government.

## DATA AVAILABILITY STATEMENT

All data supporting this study are presented herein or freely available as follows. The aerial photos and lidar data shown in the figures are available from MD iMAP at https://imap.maryland.gov/pages/data. All time series of discharge and turbidity at USGS gages are available at https://doi.org/10.5066/F7P55KJN . Morphometry data (transects and TS DEMs), facies maps, sediment sample data and aerial imagery supporting SfM photogrammetry are available at https://www.ncei.noaa.gov/archive/accession/0284223.

## ORCID

*Mathias J. Collins* https://orcid.org/0000-0003-4238-2038
*Matthew J. Cashman* https://orcid.org/0000-0002-6635-4309

## REFERENCES

AgiSoft PhotoScan Professional (Version 1.2.6) (Software). (2016). Retrieved from http://www.agisoft.com/downloads/installer/

Armstrong, W.H., Collins, M.J. & Snyder, N.P. (2014) Hydroclimatic flood trends in the northeastern United States and linkages with large-scale atmospheric circulation patterns. *Hydrological Sciences Journal*, 59(9), 1636–1655. Available from: https://doi.org/10.1080/02626667.2013.862339

Beck, H.E., Zimmermann, N.E., McVicar, T.R., Vergopolan, N., Berg, A. & Wood, E.F. (2018) Present and future Köppen–Geiger climate classification maps at 1-km resolution. *Scientific Data*, 5(1), 180214. Available from: https://doi.org/10.1038/sdata.2018.214

Belletti, B., Garcia de Leaniz, C., Jones, J., Bizzi, S., Börger, L., Segura, G., et al. (2020) More than one million barriers fragment Europe's rivers. *Nature*, 588(7838), 436–441. Available from: https://doi.org/10.1038/s41586-020-3005-2

Bellmore, J.R., Duda, J.J., Craig, L.S., Greene, S.L., Torgersen, C.E., Collins, M.J., et al. (2017) Status and trends of dam removal research in the United States. *Wiley Interdisciplinary Reviews: Water*, 4(2), e1164. Available from: https://doi.org/10.1002/wat2.1164

Bellmore, J.R., Pess, G.R., Duda, J.J., O'Connor, J.E., East, A.E., Foley, M.M., et al. (2019) Conceptualizing ecological responses to dam removal: if you remove it, what's to come? *Bioscience*, 69(1), 26–39. Available from: https://doi.org/10.1093/biosci/biy152

Bountry, J.A., Lai, Y.G. & Randle, T.J. (2013) Sediment impacts from the Savage Rapids Dam removal, Rogue River, Oregon. *Reviews in Engineering Geology*, 21, 93–104. Available from: https://doi.org/10.1130/2013.4121(08)

Cashman, M.J., Gellis, A.C., Boyd, E., Collins, M.J., Anderson, S.W., McFarland, B.D., et al. (2021) Channel response to a dam-removal sediment pulse captured at high-temporal resolution using routine gage data. *Earth Surface Processes and Landforms*, 46(6), 1145–1159. Available from: https://doi.org/10.1002/esp.5083

Christianson, J. (2016). "Bloede Dam." Written Historical and Descriptive Data, Historic American Engineering Record, National Park Service, U.S. Department of the Interior. From Prints and Photographs Division, Library of Congress (HAER No. MD-189; http://lcweb2.loc.gov/master/pnp/habshaer/md/md2000/md2053/data/md2053data.pdf, accessed July 12, 2023).

Collins, M.J. (2019) River flood seasonality in the Northeast United States: characterization and trends. *Hydrological Processes*, 33(5), 687–698. Available from: https://doi.org/10.1002/hyp.13355

Collins, M.J., Snyder, N.P., Boardman, G., Banks, W.S.L., Andrews, M., Baker, M.E., et al. (2017) Channel response to sediment release: insights from a paired analysis of dam removal. *Earth Surface Processes and Landforms*, 42(11), 1636–1651. Available from: https://doi.org/10.1002/esp.4108

Costa, J.E. (1975) Effects of agriculture on erosion and sedimentation in the Piedmont province, Maryland. *Geological Society of America Bulletin*, 86(9), 1281–1286. Available from: https://doi.org/10.1130/0016-7606(1975)86<1281:EOAOEA>2.0.CO;2

Ding, L., Chen, L., Ding, C. & Tao, J. (2019) Global trends in dam removal and related research: a systematic review based on associated datasets and bibliometric analysis. *Chinese Geographical Science*, 29(1), 1–12. Available from: https://doi.org/10.1007/s11769-018-1009-8

Doyle, M.W., Stanley, E.H., Havlick, D.G., Kaiser, M.J., Steinbach, G., Graf, W.L., et al. (2008) Aging infrastructure and ecosystem restoration. *Science*, 319(5861), 286–287. Available from: https://doi.org/10.1126/science.1149852

East, A.E. & Grant, G.E. (2023) A watershed moment for western U.S. dams. *Water Resources Research*, 59(10), e2023WR035646. Available from: https://doi.org/10.1029/2023WR035646

East, A.E., Logan, J.B., Mastin, M.C., Ritchie, A.C., Bountry, J.A., Magirl, C.S., et al. (2018) Geomorphic evolution of a gravel-bed river under sediment-starved versus sediment-rich conditions: river response to the world's largest dam removal. *Journal of Geophysical Research: Earth Surface*, 123(12), 3338–3369. Available from: https://doi.org/10.1029/2018JF004703

England, J.F., Jr., Cohn, T.A., Faber, B.A., Stedinger, J.R., Thomas, W.O., Jr., Veilleux, A.G., et al. (2019) Guidelines for determining flood flow frequency—Bulletin17C: U.S. *Geological Survey Techniques and Methods*, book4, chap. B5, 1–148, Available from: https://doi.org/10.3133/tm4B5

Ferrer-Boix, C., Martín-Vide, J.P. & Parker, G. (2014) Channel evolution after dam removal in a poorly sorted sediment mixture: experiments and numerical model. *Water Resources Research*, 50(11), 8997–9019. Available from: https://doi.org/10.1002/2014WR015550

Foley, M.M., Bellmore, J.R., O'Connor, J.E., Duda, J.J., East, A.E., Grant, G.E., et al. (2017) Dam removal—listening in. *Water Resources Research*, 53(7), 5229–5246. Available from: https://doi.org/10.1002/2017WR020457

Gilet, L., Gob, F., Virmoux, C., Gautier, E., Thommeret, N. & Jacob-Rousseau, N. (2021) Morpho-sedimentary dynamics associated to dam removal. The Pierre Glissotte dam (central France). *Science of the Total Environment*, 784, 147079. Available from: https://doi.org/10.1016/j.scitotenv.2021.147079

Graf, W.L. (2006) Downstream hydrologic and geomorphic effects of large dams on American rivers. *Geomorphology*, 79(3), 336–360. Available from: https://doi.org/10.1016/j.geomorph.2006.06.022

Gran, K.B., Montgomery, D.R. & Halbur, J.C. (2011) Long-term elevated post-eruption sedimentation at Mount Pinatubo, Philippines. *Geology*, 39(4), 367–370. Available from: https://doi.org/10.1130/G31682.1

Harrison, L.R., East, A.E., Smith, D.P., Logan, J.B., Bond, R.M., Nicol, C.L., et al. (2018) River response to large-dam removal in a Mediterranean hydroclimatic setting: Carmel River, California, USA. *Earth Surface Processes and Landforms*, 43(15), 3009–3021. Available from: https://doi.org/10.1002/esp.4464

Ibisate, A., Ollero, A., Ballarín, D., Horacio, J., Mora, D., Mesanza, A., et al. (2016) Geomorphic monitoring and response to two dam removals: rivers Urumea and Leitzaran (Basque Country, Spain). *Earth Surface Processes and Landforms*, 41(15), 2239–2255. Available from: https://doi.org/10.1002/esp.4023

Itsukushima, R., Ohtsuki, K., Sato, T., Kano, Y., Takata, H. & Yoshikawa, H. (2019) Effects of sediment released from a check dam on sediment deposits and fish and macroinvertebrate communities in a small stream. *Water*, 11(4), 716. Available from: https://doi.org/10.3390/w11040716

James, M.R., Robson, S., d'Oleire-Oltmanns, S. & Niethammer, U. (2017) Optimising UAV topographic surveys processed with structure-from-motion: ground control quality, quantity and bundle adjustment. *Geomorphology*, 280, 51–66. Available from: https://doi.org/10.1016/j.geomorph.2016.11.021

Lehner, B., Liermann, C.R., Revenga, C., Vörösmarty, C., Fekete, B., Crouzet, P., et al. (2011) High-resolution mapping of the world's reservoirs and dams for sustainable river-flow management. *Frontiers in Ecology and the Environment*, 9(9), 494–502. Available from: https://doi.org/10.1890/100125

Major, J.J., East, A.E., O'Connor, J.E., Grant, G.E., Wilcox, A.C., Magirl, C.S., et al. (2017) Geomorphic responses to dam removal in the United States—a two-decade perspective. In: *Gravel-bed rivers: processes and disasters*. West Sussex, UK: Wiley and Sons, pp. 355–383 https://doi.org/10.1002/9781118971437.ch13

Major, J.J., O'Connor, J.E., Podolak, C.J., Keith, M.K., Grant, G.E., Spicer, K.R., et al. (2012) Geomorphic response of the Sandy River, Oregon, to removal of Marmot Dam. *U.S. Geological Survey Professional Paper*, 1792, 1–64, Available from: https://pubs.usgs.gov/pp/1792/.and data tables at

Major, J.J., Zheng, S., Mosbrucker, A.R., Spicer, K.R., Christianson, T. & Thorne, C.R. (2019) Multidecadal geomorphic evolution of a profoundly disturbed gravel bed river system—a complex, nonlinear response and its impact on sediment delivery. *Journal of Geophysical Research: Earth Surface*, 124(5), 1281–1309. Available from: https://doi.org/10.1029/2018JF004843

Maryland Department of Natural Resources Watershed Services (MDNRWS). (2005) *Characterization of the Patapsco River Lower North Branch Watershed in Howard County*. Annapolis, Maryland: MDNRWS, p. 21.

Mulligan, M., Lehner, B., Zarfl, C., Thieme, M., Beames, P., van Soesbergen, A., et al. (2021) Global Dam Watch: curated data and tools for management and decision making. *Environmental Research: Infrastructure and Sustainability*, 1(3), 033003.

Nagayama, S., Ishiyama, N., Seno, T., Kawai, H., Kawaguchi, Y., Nakano, D., et al. (2020) Time series changes in fish assemblages and habitat structures caused by partial check dam removal. *Water*, 12(12), 3357. Available from: https://doi.org/10.3390/w12123357

National Weather Service. (2023). Advanced Hydrologic Prediction Service. Retrieved June 2023 from https://water.weather.gov/ahps2/hydrograph.php?wfo=lwx&gage=erdm2&prob_type=stage&source=hydrograph

Pearson, A.J. & Pizzuto, J. (2015) Bedload transport over run-of-river dams, Delaware, USA. *Geomorphology*, 248, 382–395. Available from: https://doi.org/10.1016/j.geomorph.2015.07.025

Pearson, A.J., Snyder, N.P. & Collins, M.J. (2011) Rates and processes of channel response to dam removal with a sand-filled impoundment. *Water Resources Research*, 47(8), W08504. Available from: https://doi.org/10.1029/2010WR009733

Petts, G.E. (1984) *Impounded rivers: perspectives for ecological management*. Chichester: Wiley.

Randle, T.J., Bountry, J.A., Ritchie, A. & Wille, K. (2015) Large-scale dam removal on the Elwha River, Washington, USA: erosion of reservoir sediment. *Geomorphology*, 246, 709–728. Available from: https://doi.org/10.1016/j.geomorph.2014.12.045

Sauer, V.B. (2001) Standards for the analysis and processing of surface-water data and information using electronic methods. *US Geological Survey Water-Resources Investigations Report*, 2001–4044, 91p. Available from: https://doi.org/10.3133/wri20014044

Smith, J.A., Baeck, M.L., Villarini, G. & Krajewski, W.F. (2010) The hydrology and hydrometeorology of flooding in the Delaware River Basin. *Journal of Hydrometeorology*, 11(4), 841–859. Available from: https://doi.org/10.1175/2010JHM1236.1

Smith, J.A., Villarini, G. & Baeck, M.L. (2011) Mixture distributions and the hydroclimatology of extreme rainfall and flooding in the eastern United States. *Journal of Hydrometeorology*, 12(2), 294–309. Available from: https://doi.org/10.1175/2010JHM1242.1

Stillwater Sciences. (2014). Sediment transport in the Patapsco River, Maryland following Bloede Dam removal. Technical Memorandum, prepared for American Rivers, 1101 14th St. NW. Suite 1400, Washington, DC 20005, 43 pages, September 20.

Synergics, Inc. (1989). Alternative solutions for Bloede Dam at Patapsco Valley State Park. State of Maryland Project No. P-020-891-001. Annapolis, MD, 72 pages.

Taylor, J.R. (1997) *An introduction to error analysis*. Sausalito, CA: University Science Books.

Tullos, D.D., Collins, M.J., Bellmore, J.R., Bountry, J.A., Connolly, P.J., Shafroth, P.B., et al. (2016) Synthesis of common management concerns associated with dam removal. *Journal of the American Water Resources Association (JAWRA)*, 52(5), 1179–1206. Available from: https://doi.org/10.1111/1752-1688.12450

Turnipseed, D.P. & Sauer, V.B. (2010) Discharge measurements at gaging stations. *US Geological Survey Techniques and Methods*, book 3, chap. A8, 87p. Available from: https://doi.org/10.3133/TM3A8

Van Ryswick, S., Sylvia, E.R., Knippler, K.A., Gillmor, A., & Connallon, C. (2017). Physical monitoring and sediment mapping survey of the Patapsco River near Bloede Dam, Howard and Baltimore Counties, Maryland. Coastal and Estuarine Geology File Report No. 16–07. Baltimore, MD, 25 pages. Retrieved June 2023 from http://www.mgs.md.gov/publications/report_pages/FR_16-07.html

Veilleux, A.G., Cohn, T.A., Flynn, K.M., Mason Jr, R.R., & Hummel, P.R. (2014). *Estimating magnitude and frequency of floods using the PeakFQ 7.0 program*. US Geological Survey: Reston, VA, USA. https://doi.org/10.3133/fs20133108

Wagner, R.J., Boulger Jr, R.W., Oblinger, C.J., & Smith, B.A. (2006). Guidelines and standard procedures for continuous water-quality monitors: station operation, record computation, and data reporting. US Geological Survey Techniques and Methods No. 1-D3, 96 p., accessed March 20,224 at https://pubs.usgs.gov/tm/2006/tm1D3/

Winter, J.M., Huang, H., Osterberg, E.C. & Mankin, J.S. (2020) Anthropogenic impacts on the exceptional precipitation of 2018 in the mid-Atlantic United States. *Bulletin of the American Meteorological Society*, 101(1), S5–S10. Available from: https://doi.org/10.1175/BAMS-D-19-0172.1

Wolman, M.G. & Miller, J.P. (1960) Magnitude and frequency of forces in geomorphic processes. *Journal of Geology*, 68(1), 54–74. Available from: https://doi.org/10.1086/626637

Woodget, A.S., Carbonneau, P.E., Visser, F. & Maddock, I.P. (2015) Quantifying submerged fluvial topography using hyperspatial resolution UAS imagery and structure from motion photogrammetry. *Earth Surface Processes and Landforms*, 40(1), 47–64. Available from: https://doi.org/10.1002/esp.3613

## Data citations

[dataset] MD iMAP. (2023a). Baltimore and Howard County LiDAR data available on the World Wide Web (LiDAR Topography Server), last accessed July 13, 2023, at https://imap.maryland.gov/pages/lidar-topography-server

[dataset] MD iMAP. (2023b). Six inch resolution aerial imagery for the State of Maryland available on the World Wide Web (MD_SixInchImagery [MapServer]), last accessed June 12, 2023, at https://geodata.md.gov/imap/rest/services/Imagery/MD_SixInchImagery/MapServer

[dataset] MD iMAP. (2023c). Six inch resolution aerial imagery for the State of Maryland available on the World Wide Web (SixInchImagery2014_2016 [MapServer]), last accessed June 02, 2023, at https://imagery.geodata.md.gov/imap/rest/services/SixInch/SixInchImagery2014_2016/MapServer

[dataset] NOAA. (2023). United States 1991–2020 climate normal; accessed at http://www.ncdc.noaa.gov/cdo-web/datatools/normals

[dataset] U.S. Geological Survey (USGS). (2023). USGS water data for the Nation: U.S. Geological Survey National Water Information System database, accessed June 02, 2023, at https://doi.org/10.5066/F7P55KJN

## SUPPORTING INFORMATION

Additional supporting information can be found online in the Supporting Information section at the end of this article.

**How to cite this article:** Collins, M.J., Baker, M.E., Cashman, M.J., Miller, A. & Van Ryswick, S. (2024) Impounded sediment and dam removal: Erosion rates and proximal downstream fate. *Earth Surface Processes and Landforms*, 1–14. Available from: https://doi.org/10.1002/esp.5850